Nanoparticle Enlarged Interfacial Effect on Phase Transition of 1-Octadecanol/Silica Composites

ARTICLE *in* THE JOURNAL OF PHYSICAL CHEMISTRY B · JANUARY 2015

Impact Factor: 3.3 · DOI: 10.1021/jp512124s · Source: PubMed

THE JOURNAL OF PHYSICAL CHEMISTRY B

Article

pubs.acs.org/JPCB

Nanoparticle Enlarged Interfacial Effect on Phase Transition of 1-Octadecanol/Silica Composites

Xia Gao, Baoquan Xie, Yunlan Su,* Dongsheng Fu, and Dujin Wang*

Beijing National Laboratory for Molecular Sciences, Key Laboratory of Engineering Plastics, Institute of Chemistry, Chinese Academy of Sciences, No. 2, North Street 1, Zhongguancun, Beijing 100190, China

ABSTRACT: Motivated by the interest in an interfacial effect on crystallization behaviors and material properties of polymer nanocomposites, phase behaviors of a novel model system for polymer nanocomposite, 1-octadecanol/silica nanosphere composites ($C_{18}OH/SiO_2$), were studied by means of thermal analysis and wide-angle X-ray diffraction. Although a huge specific surface area of silica nanoparticles enlarges the surface−volume ratio of $C_{18}OH$ molecules, surface freezing phenomenon is not observed by DSC in the $C_{18}OH/SiO_2$ composites. While pure $C_{18}OH$ exhibits rotator R_{IV} phase with molecules tilted with respect to the layer normal, the silica network favors and enhances untitled R_{II} phase by disturbing the layering arrangement. Moreover, the confined $C_{18}OH$ shows a polycrystalline mixture of orthorhombic β form and monoclinic γ form. It is demonstrated that the interfacial interaction between the $C_{18}OH$ molecules and the silica surface contributes to the peculiar phase transition behaviors of $C_{18}OH/SiO_2$ composites. The investigation of the model system of long-chain alcohol/nano-SiO_2 composites may help us to understand the complicated interfacial effect on phase behaviors and material properties of polymer nanocomposite systems.

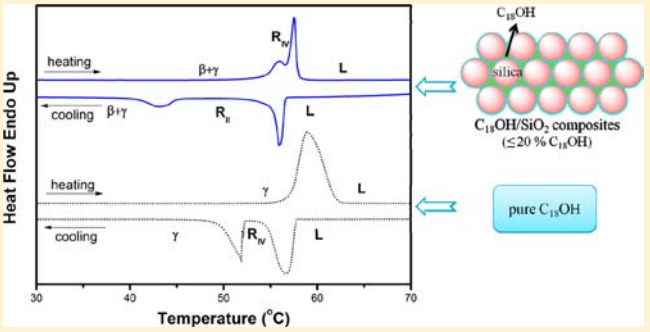

INTRODUCTION

Polymer nanocomposites (PNCs), with nanofillers dispersed in polymer matrix, can cope with some limitations of pure polymer materials and enhance the mechanical and barrier properties of materials.[1,2] In the past two decades, many works have been devoted to understanding the underlying enhancement mechanism for PNCs, which is a key point for design of composite and property-enhancing modification for traditional materials. In PNC systems using three-dimensional nanoparticles as the filler, the interfacial effect is believed to be the main reason for affecting the properties of PNCs. Due to the huge specific surface area of nanoparticles, a significant portion of polymer is located at the interfacial region between nanoparticle surface and polymer matrix. In the interfacial region, interactions (attractive or repulsive) between nanoparticles and polymer alter the local segment dynamics of polymer chains drastically through modifying packing density, chain conformation, and orientation, and further the structure and properties of interfacial layer exert a substantial effect on the overall properties of the nanocomposite.[3−8] As reported, attractive interaction results in an immobilized polymer layer near the nanoparticle surface, and thus a higher T_g,[5,9] whereas repulsive interaction reduces the obstruction of polymer chain movement, and thereby results in a lower T_g.[10] A core−two-shell model is proposed to elucidate the different dynamics between interfacial and bulk polymer. The core is the nanoparticle, and the inner shell is the interfacial region where polymer segments are modified in molecular mobility, while the outer shell is the bulk region where polymer chains exhibit the same behaviors as bulk polymer chains.[4,11−13] The changes from interfacial to bulk properties take place in a gradual fashion over the width of the interfacial region. Nevertheless, due to the complexity of molecular structure, molecular weight distribution, as well as the polymorphism, metastability, and confinement effect in polymer nanocomposite system, until now there is no universal conclusion between properties of polymer nanocomposites and local segment and long-range chain dynamics in the interfacial region, which to some extent inhibits precise design and industrial application of polymer nanocomposites.[14]

In our previous work,[15,16] a model polymer nanocomposite system with weak interfacial interaction between fillers and matrix, *n*-alkane/SiO_2 composite, was developed by mixing alkane melt and silica particles. As evident from DSC measurement, the surface freezing phenomenon of alkane is enhanced in the composite, similar to what occurred in three-dimensional microencapsulated *n*-alkanes.[17] Furthermore, *n*-alkane has been found to be efficiently confined in the surface region of nanoparticles and the interspace region of particle aggregates, where the crystallization behavior of *n*-C_{19} is significantly different from that of bulk.[15] Various experiments and phenomenological theories by other groups also demonstrated that nanosilica networks exhibit significant influence on phase transitions in tetracosane.[18−20] The phase

Received: December 5, 2014
Revised: January 9, 2015
Published: January 12, 2015

DOI: 10.1021/jp512124s
J. Phys. Chem. B 2015, 119, 2074−2080

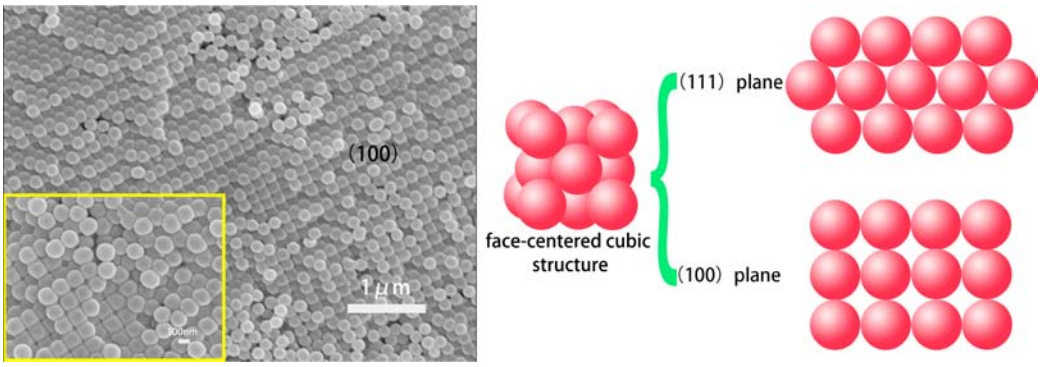

Figure 1. SEM images of $C_{18}OH/SiO_2$ (150 nm) composites with $\varphi_{C18OH} \leq 20\%$. For convenience, the schematic illustration of FCC structure and the silica arrangement in (100) and (111) planes are given in the right cartoon. Composites with different silica size (350 and 90 nm in diameters) also demonstrate an FCC structure, and the results are not shown here.

transition temperature of *n*-alkanes near the silica surface shifts downward with respect to that of its pure counterpart. Over the R_I-R_V transition, where it has a first-order character in pure alkanes, the disorder introduced by silica network tends to weaken it toward a second-order character. In this regard, *n*-alkane/SiO_2 composite systems not only provide a new route to investigate phase transition under confinement, but also can act as a model system for PNCs to discover the interfacial effect.

The alcohol molecule (C_nOH) is almost identical with normal alkane (C_n), the only difference being the exchange of an H on terminal methyl with a hydroxyl OH group. Due to the nature of the alkyl chain, C_nOH also shows a similar surface freezing phenomenon,[21] rotator phase, and phase sequence as *n*-alkanes.[22,23] However, the hydroxyl groups give them unique properties, and hydrogen bonds between adjacent molecules play an important role in determining crystal structure and thereby phase transition temperature of *n*-alcohols.[22,23] In terms of surface freezing, only those with an even carbon number show surface bilayer with the hydroxyl groups of the upper and lower layers pointing to the center of the bilayer,[21] unlike alkanes, where a surface monolayer occurs for both odd and even carbon number.[24] When mixed with hydrophilic silica nanopaticles, C_nOH molecules can form hydrogen bond with silanol on the silica surface, which would exert an essential effect on the phase transition of *n*-alcohols, compared to the weak van der Waals interaction in *n*-alkane/silica composites.

Therefore, in this work, a new polymer nanocomposite model system, 1-octadecanol ($C_{18}OH$)/SiO_2, is developed to investigate composites with strong interfacial interaction. To well assess the interfacial effect of silica nanoparticles on the crystallization of $C_{18}OH$, composites were prepared by solution mixing method[5,25] to ensure the homogeneity of samples. The crystallization behaviors of pure $C_{18}OH$ and $C_{18}OH/SiO_2$ composites were investigated by differential scanning calorimetry (DSC) and synchrotron radiation wide-angle X-ray scatting (WAXS). As expected, phase transition behavior of $C_{18}OH$ molecules in composites is significantly different from that of pure $C_{18}OH$. Furthermore, unlike the case in *n*-alkane/SiO_2 composites, surface freezing phenomenon has not been observed in $C_{18}OH/SiO_2$ composites. Also, the underlying reasons are explored and discussed in this work.

EXPERIMENTAL SECTION

1-Octadecanol ($C_{18}OH$) with purity 99% was purchased from Sigma-Aldrich Co., and was used as received. The spherical silica nanoparticles with a dispersion less than 5% were synthesized following the Stöber method.[26] Through strict control of reaction conditions, SiO_2 nanoparticles with a diameter ranging from 90 to 650 nm can be obtained. Also, the sizes of silica used here were 350, 150, and 90 nm in diameters. Taking into account of the complexity of *in situ* polymerization, which introduces the chemical bond and grafting density, the solution mixing is used here for homogeneity. $C_{18}OH$ and nanoparticles were separately dispersed in ethanol and bath-sonicated for 15 min, and then mixed by desired volume ratio. After stirring for 48 h at room temperature, samples were obtained by evaporating solvent at atmospheric environment and then dried in a vacuum oven for 48 h at 45 °C to remove the residual solvent.

The morphology of composite samples was examined by a JEOL-JSM-6700F scanning electron microscope fitted with a field emission source and operated at an accelerating voltage of 10 kV. Differential scanning calorimetry (DSC) measurements were performed with a Q2000 (TA Instruments) in the temperature range 20−80 °C at a rate of 2 °C/min under nitrogen atmosphere. The transition temperatures and heat capacities were calculated via TA Universal Analysis 2000 software.

In situ X-ray scattering measurements were carried out at the beamline 14 B in Shanghai Synchrotron Radiation Facility (SSRF). A Linkam thermal stage was used for temperature control. The wavelength of radiation source was 1.24 Å. WAXS patterns were collected by a Mar CCD with a resolution of 3072 × 3072 pixels (pixel size: 79 × 79 mm^2). Image acquisition time was 30 s. The sample to detector distance was 368 mm.

Solid ^{13}C NMR experiments were performed on a 400 MHz Bruker Avance III at ^{13}C Larmor frequency of 100.38 MHz. Samples were contained in a cylindrical 4 mm rotor made of zirconia at room temperature (at which all samples crystallize into their low-temperature crystal structures). The pulse program CPTOSS was used to obtain the NMR spectra of adsorbed molecules on the silica surface. Also, the contact time was 3 ms.

RESULTS AND DISCUSSION

SEM morphology of the $C_{18}OH/SiO_2$ composite with 20 wt % $C_{18}OH$ is shown in Figure 1. It has been experimentally evidenced that Stöber SiO_2 nanospheres with diameters ranging from 50 to 500 nm arrange in a crystalline face-centered cubic (FCC) structure through natural sedimentation driven by the

DOI: 10.1021/jp512124s
J. Phys. Chem. B 2015, 119, 2074−2080

minimum energy.[27] Also, the FCC structure was reported in silica and silver nanoparticles stabilized by long chain alkane molecules.[28,29] Upon solvent evaporation, the gradually increasing repulsion induced by the adsorbed alkane chains balances well with the attraction among silica nanoparticles, ensuring that the entropically favored FCC structure is formed. With the hydroxyl groups of alcohol molecules interacting with the silanol groups on the silica surfaces by forming hydrogen bonds, the long alkyl chains still play an important role in stabilizing the FCC structure. As shown in Figure 1, the characteristic (100) plane of the FCC structure is observed in the composites where the mass ratio of $C_{18}OH$ (φ_{C18OH}) is less than 20%. Obviously, for $C_{18}OH/SiO_2$ composites with a high SiO_2 content, *n*-alcohol is homogeneously dispersed into the interspace between SiO_2 nanospheres. In the FCC structure, both the interfacial region and the interspace between neighbor nanoparticles are on the size order of nanometers,[15,30] which may exert an essential confinement effect on crystallization of $C_{18}OH$.

Multiple Phase Transition Behaviors in $C_{18}OH/SiO_2$ Composites. Figure 2 shows the crystallization behaviors of pure $C_{18}OH$ and $C_{18}OH/SiO_2$ (350 nm) composites. Pure $C_{18}OH$ undergoes a liquid−solid transition at 57 °C and then a solid−solid transition at 52 °C during cooling process. When silica nanoparticles are mixed with $C_{18}OH$, the crystallization behaviors of composites are different from that of pure $C_{18}OH$, demonstrated by a new small exothermic peak appearing at 42 °C for the specimen with $\varphi_{C18OH} \leq 70$ wt %. According to previous reports, the silica network can provide transitional disorders for adsorbed alkane molecules and favor the formation of gauche conformation at chain-ends, which contributes to weaken the interlayer coupling and thereby enhances the stability of rotator phase.[15,16,18−20] Therefore, the solid−solid transition of alkane in composites tends to occur at a lower temperature than that of pure sample. Reasonably, the peak at 42 °C can be attributed to the confined solid−solid transition of $C_{18}OH$. Obviously, the temperature range over which the rotator phase is stable is significantly increased, changing from 5 °C in pure sample up to 14 °C in the composites. For comparison, the two peaks, appearing at the liquid−rotator transition temperature and the rotator−crystal transition temperature of pure $C_{18}OH$, are referred to as bulk liquid−solid transition and bulk solid−solid transition, respectively, as indicated by arrows in Figure 2. With the content of $C_{18}OH$ decreasing from 50 to 30 wt %, the peak intensity of confined solid−solid transition becomes stronger and stronger. Meanwhile, the liquid−solid transition splits into two peaks, with the one at higher temperature (57 °C) corresponding to the bulk liquid−solid transition and the other at 56 °C possibly arising from the liquid−solid transition of confined $C_{18}OH$. Upon further decreasing φ_{C18OH} to 20 wt %, only the one at 56 °C and the other one attributed to the confined solid−solid transition peak (~42 °C) appear on the DSC curves, whereas both the bulk liquid−solid (57 °C) and bulk solid−solid transition (52 °C) peaks disappear. Under the high content of silica nanoparticles, the alcohol molecules are dispersed on the silica surfaces, and the interspaces of FCC structure are shown in SEM image (Figure 1), where the silica network exerts confinement effect on the crystallization of $C_{18}OH$ molecules, demonstrated by the lower liquid−solid transition and solid−solid transition temperatures as compared to those of pure $C_{18}OH$. Here, the exothermic peak at 56 °C arises from the confined liquid−rotator transition for the composites with $\varphi_{C18OH} \leq 20$%. To investigate the confined crystallization behavior of $C_{18}OH/SiO_2$ composites, the specimens with the content of $C_{18}OH$ below 20 wt % are chosen in the following experiments.

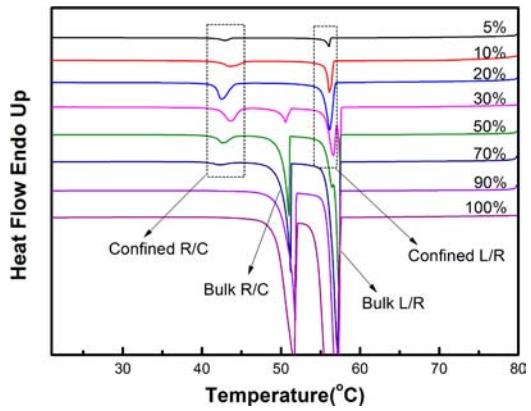

Figure 2. DSC traces of $C_{18}OH/SiO_2$ (350 nm) composites with various contents of $C_{18}OH$ during cooling processes. The percentages are for the mass ratio of $C_{18}OH$ in the composites.

"Disordered" Crystal Structures Induced by the Silica Network. To further characterize crystal structures and phase transitions more clearly, *in situ* WAXS measurements were performed on the crystallization processes of pure $C_{18}OH$ and $C_{18}OH/SiO_2$ (350 nm) composites. As shown in Figure 3A, pure $C_{18}OH$ exists as the isotropic liquid state at above 58 °C, characterized by a single halo. With temperature decreasing to 56 °C, two diffraction peaks appear which indicate the

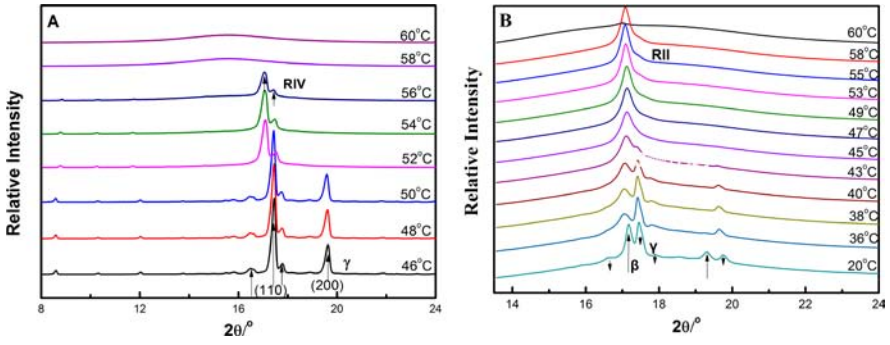

Figure 3. *In situ* WAXS profiles of pure $C_{18}OH$ (A) and $C_{18}OH/SiO_2$ (350 nm) composite with φ_{C18OH} = 20 wt % (B) (the WAXS results for composites with $\varphi_{C18OH} \leq 20$ wt % have worse signal-to-noise ratios due to the high SiO_2 content). The cooling rate was 2 °C/min.

DOI: 10.1021/jp512124s
J. Phys. Chem. B 2015, 119, 2074−2080

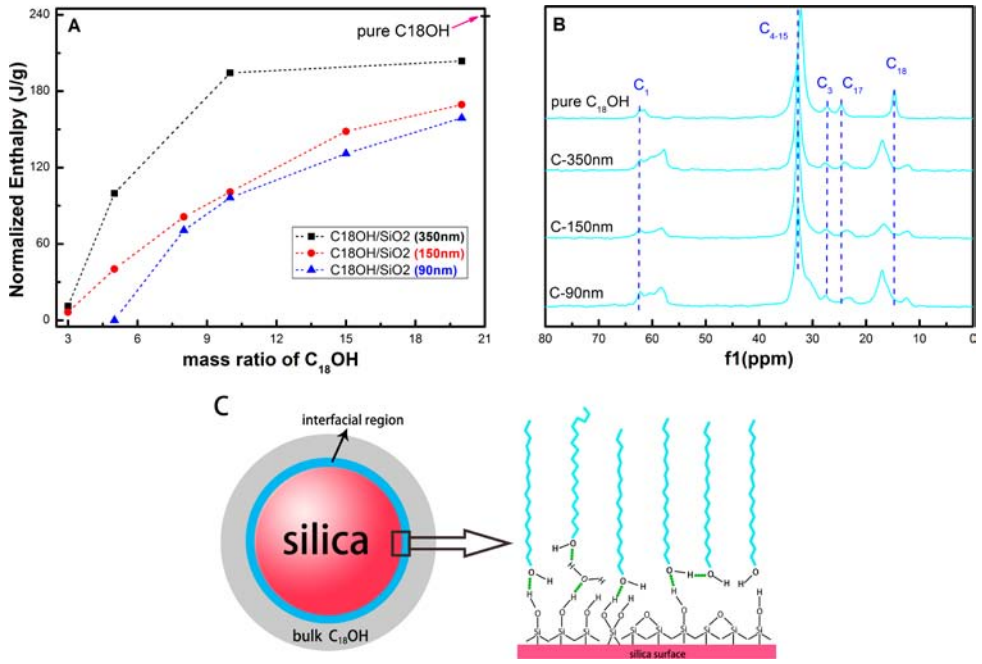

Figure 4. (A) Variation of normalized melting ($\Delta H_{melting}$) of $C_{18}OH/SiO_2$ composites with $\varphi_{C18OH} \leq 20\%$ (the diameters of silica particle investigated are 350, 150, 90 nm, respectively). (B) Solid-state ^{13}C NMR spectra of pure $C_{18}OH$ and $C_{18}OH/SiO_2$ (5% $C_{18}OH$) composites with different sizes of silica at room temperature, where C_1 is for the carbon bonded to the OH, and C_{18} is for the terminal methyl group at the other end of the chain. (C) Schematic illustration of the conformation and orientation of molecules in the interfacial region of $C_{18}OH/SiO_2$ composites. Hydrogen bonds form between the silica surface and $C_{18}OH$ molecules, favoring the translational disorder and thus rotational disorder of molecules of successive layer.

appearance of rotator phase R_{IV}. The small one at higher angle results from the molecule tilted with respect to the layer normal in R_{IV}.[30,31] Upon further cooling pure $C_{18}OH$ to below 50 °C, four characteristic diffraction peaks emerge, corresponding to the monoclinic γ phase.[32] Furthermore, higher lamellar ordering with bilayer molecules in the low-temperature crystal structure is observed, indicated by a series of equidistant Bragg peaks (00l) at low angles.

However, for the composite with 20 wt % $C_{18}OH$ and the size of silica being 350 nm in diameter, a single peak centered at 17°, which points to the hexagonal in-plane lattice, appears just below the liquid−solid transition temperature. This suggests that the composite exhibits rotator phase R_{II}, in which the long axes of molecules are perpendicular to the layer normal. As is well-known, R_{II} is the rotator phase with highest degree of rotational disorder and end-gauche defects, while R_{IV} phase has monolayer stacking with molecules tilted toward next-nearest neighbors.[22,23,33] If the transitional and rotational disorders of molecules are enhanced by chain mixing or other random strain, R_{II} phase will be stabilized over R_{IV} phase due to the weakened interlayer coupling.[34−36] As reported,[18−20] the silica network favors the formation of gauche defects at the chain-ends and thus rotational disorder of long-chain molecules. Therefore, the more disordered R_{II} phase occurs in the composites instead of R_{IV} phase. Also, it is noteworthy that the diffraction peak of the rotator phase is always asymmetric, and there is some nonresolved peak splitting,[35] which arises from the residual tilted molecules observed in the R_{IV} phase of pure $C_{18}OH$. Upon further decreasing the temperature to 20 °C, both the characteristic diffraction peaks of orthorhombic phase β phase and the monoclinic γ phase coexist at lower temperature. This indicates that the low-temperature crystal structure of $C_{18}OH/SiO_2$ composites with 20 wt % $C_{18}OH$ is the coexistence of β phase and γ phase. The reason will be discussed in detail below.

Interfacial Effect of Silica Nanoparticles in the Composites. Multiple phase transition behaviors have also been reported in C_{19}/SiO_2 composites.[15] Moreover, C_{19}/SiO_2 composites exhibit enhanced surface freezing as the same case in microencapsulated *n*-alkanes.[17] Because the weak van der Waals force dominates the interaction between amorphous silica surfaces and nonpolar alkane molecules in the interface, this interaction is not strong enough to collapse the surface monolayer, which is stabilized by the lateral intermolecular interaction.[24,37] Therefore, surface freezing can still occur with alkane molecules "standing" on the surfaces of silica nanoparticles. In addition, due to the huge specific surface area of SiO_2 nanoparticles, the surface-to-volume ratio of surface molecules is dramatically enlarged (for example, ∼14% of total molecules for the alkane/SiO_2 (350 nm) = 10/90 composite standing on the interface between liquid alkanes and silica surface). This makes it possible that the surface freezing heat is large enough to be detected by the normal DSC methods. However, surface freezing phenomenon could not be observed by DSC in $C_{18}OH/SiO_2$ composites. Generally, pure $C_{18}OH$ exhibits a surface bilayer with the hydroxyl groups of the upper and lower layers pointing to the center of the bilayer at ∼1 °C above the crystallization temperature. Also, hydrogen bond interaction dominates the stability of the surface bilayer. In the $C_{18}OH/SiO_2$ composites with φ_{C18OH} < 20 wt %, due to the huge specific surface area and thus large surface energy of silica nanoparticles, there is an adsorbed layer (interfacial region) close to the silica surface with the hydroxyl group interacting with the silanol group. As calculated by the normalized melting enthalpy $\Delta H_{melting}$ in Figure 4A, the amount of adsorbed $C_{18}OH$ increases with decrease of

DOI: 10.1021/jp512124s
J. Phys. Chem. B 2015, 119, 2074−2080

nanoparticle size, from 0.042 g of $C_{18}OH$/g SiO_2 for 350 nm, to 0.054 g of $C_{18}OH$/g SiO_2 for 150 nm and to 0.057 g of $C_{18}OH$/g SiO_2 for 90 nm. Also, the thickness of the adsorbed layer is calculated to be 3−4 nm, close to the chain length of all-*trans* $C_{18}OH$ molecule (2.5 nm). In Figure 4B, the solid ^{13}C NMR spectra of pure $C_{18}OH$ and $C_{18}OH/SiO_2$ (5% $C_{18}OH$) composites at room temperature are shown to elucidate the molecular dynamics and conformation of adsorbed molecules in the interfacial region. The chemical shift of the C_{18} (the terminal methyl group) peak moves upfield by 0.5 ppm compared to that of pure sample, meaning the methyl groups of $C_{18}OH$ molecules in the interfacial region are undergoing relatively fast transition between *trans* and *gauche* conformations.[38] However, the chemical shift of the int-CH_2 (C_{4-15}) peak is nearly identical for both pure $C_{18}OH$ and $C_{18}OH/SiO_2$ composites, which suggests that the adsorbed molecules exhibit the same lateral interaction between molecules as pure $C_{18}OH$ (in crystal form). Therefore, in the interfacial region, $C_{18}OH$ molecules are adsorbed on the silica surface with the hydroxyl groups interacting with silanol groups and the long alkyl chains extending out or standing on, as shown in the cartoon of Figure 4C. This result is consistent with the case for $C_{18}OH$ adsorbed on the planar sapphire surface, where X-ray studies reveal that the monolayer formed at the bulk melt alkanol−sapphire interface is densely packed with $C_{18}OH$ hydrogen bound to the sapphire and their long axes normal to the surface.[39] In this regard, there is no chance for the molecules in successive layers to form hydrogen bond with these adsorbed molecules. On the other hand, since the amorphous silica surface is rough, these adsorbed molecules exhibit enhanced translational disorder, which can be easily translated to other molecules and further disturbs the formation of hydrogen bond between adsorbed layer and other successive layers. Altogether, though silica nanoparticles in this work possess a huge specific surface area, silica nanoparticles suppress the formation of an ordered bilayer in the interfacial region; therefore, the enhanced surface freezing phenomenon could not be observed in $C_{18}OH/SiO_2$ composites.

For pure *n*-alcohols, there are two kinds of low-temperature crystal structures. The γ phase is an ordered form with a monoclinic symmetry in which all C−C bonds of the molecules have the *trans* conformation, occurring in even *n*-alcohols. Whereas the β phase contains two molecules in the unit cell, the first isomer is an all-*trans* conformer while the second has the C−C−C−O torsion angle in gauche form.[22,23,31] In $C_{18}OH/SiO_2$ composites, two crystal structures β and γ phases coexist. As mentioned above, $C_{18}OH$ molecules near the silica surface exhibit the weakened hydrogen bond interaction between upper and lower layers and the enhanced translational disorder of molecules. Also, this kind of disorder introduced by the solid surface cannot be eliminated with temperature decreasing. Furthermore, the interspace of the FCC structure is randomly connected, which will essentially enhance the rotational and translational disorder of molecules. As a result, the layer-by-layer structures are suppressed in the composites, indicated by the absence of (00*l*) series diffraction peaks at low Bragg angle in Figure 3B. Therefore, R_{II} tends to translate to β phase with gauche defect at chain-ends at lower temperature. However, the farther the molecules are away from the silica surface, the weaker the interaction between silica surface and molecules is, and thereby the weaker the effect on the translational degree-of-freedom is. Molecules far away from silica surface act as in bulk state as shown in Figure 4C and can still exhibit γ phase with strong interlayer coupling. Altogether, the low-temperature crystal structure of the composite with φ_{C18OH} = 20% exhibits the coexistence of β phase and γ phase.

As is well-known, the profound hydrogen bond interaction between adjacent *n*-alcohol molecules induces the significant higher crystallization and melting temperatures than those of alkane with the same carbon number.[21] The transition temperature of hydrated alcohol is also higher than that of dry alcohol, since the interaction is increased by ~5 kJ/mol due to the enhancement of hydrogen bond with water molecule intercalation.[21,22] However, the occurrence of silica nanoparticles exerts influence on the interaction between adjacent $C_{18}OH$ molecules by introducing the translational disorder and disturbing hydrogen bond, as discussed above. Also, the disturbed hydrogen bond in crystalline structures results in the stability of β phase and the decrease of liquid−rotator transition temperature of composites compared to that of pure $C_{18}OH$, shown in Figure 5. With the size of silica decreasing

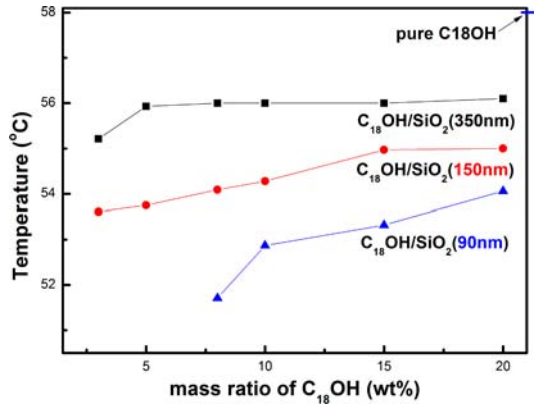

Figure 5. Liquid−rotator transition temperatures of $C_{18}OH/SiO_2$ composites with $\varphi_{C18OH} \leq 20\%$ (the liquid−rotator transition temperature of pure $C_{18}OH$ is 58 °C, indicated by the blue dot).

from 350 to 90 nm, the liquid−rotator transition temperature $T_{L/R,\,C}$ decreases from 56 to 50 °C. Under the same content of silica nanoparticles, the surface area increases with decrease of silica nanoparticle size, and thus more $C_{18}OH$ molecules are adsorbed on the surface of smaller silica nanoparticles, accordingly reducing the lower liquid−rotator temperature in the composites with smaller silica.

CONCLUSIONS

In summary, both the silica surfaces and the geometric space in the silica network induce the peculiar crystallization behavior of $C_{18}OH/SiO_2$ composites. In the interfacial region, the slightly polar $C_{18}OH$ molecules interact with the silica surface through hydrogen bonding, thus enhancing the translational disorder along the long axes of molecules and disturbing the formation of hydrogen bond between adjacent molecules. In addition, the random connected interspace essentially favors the rotational and translational disorder of $C_{18}OH$ molecules. Altogether, the silica network, especially the silica surfaces, induces the stability of untitled R_{II} phase and β phase with weakened interlayer coupling. This work is believed to highlight the effect of fillers on the properties of polymer nanocomposite.

DOI: 10.1021/jp512124s
J. Phys. Chem. B 2015, 119, 2074−2080

AUTHOR INFORMATION

Corresponding Authors

*Phone: +86-10-82618533. Fax: +86-10-82612857. E-mail: ylsu@iccas.ac.cn.

*Phone: +86-10-62556180. Fax: +86-10-82362045. E-mail: djwang@iccas.ac.cn.

Notes

The authors declare no competing financial interest.

ACKNOWLEDGMENTS

We thank the National Natural Science Foundation of China (51103166) for financial support. We also appreciate the staff scientists at beamline 14B in Shanghai Synchrotron Radiation Facility (SSRF) for beam time and technical assistance.

REFERENCES

(1) Dorigato, A. Linear Low-Density Polyethylene/Silica Micro- and Nanocomposites: Dynamic Rheological Measurements and Modelling. *eXPRESS Polym. Lett.* **2010**, *4*, 115−129.

(2) Reynaud, E.; Jouen, T.; Gauthier, C.; Vigier, G.; Varlet, J. Nanofillers in Polymeric Matrix: A Study on Silica Reinforced PA 6. *Polymer* **2001**, *42*, 8759−8768.

(3) Tsagaropoulos, G.; Eisenburg, A. Direct Observation of Two Glass Transitions in Silica-Filled Polymers. Implications to the Morphology of Random Ionomers. *Macromolecules* **1995**, *28*, 396−398.

(4) Klonos, P.; Panagopoulou, A.; Kyritsis, A.; Bokobza, L.; Pissis, P. Dielectric Studies of Segmental Dynamics in Poly(dimethylsiloxane)/Titania Nanocomposites. *J. Non-Cryst. Solids* **2011**, *357*, 610−614.

(5) Füllbrandt, M.; Purohit, P. J.; Schönhals, A. Combined FTIR and Dielectric Investigation of Poly(vinyl acetate) Adsorbed on Silica Particles. *Macromolecules* **2013**, *46*, 4626−4632.

(6) Lin, W. Y.; Blum, F. D. Segmental Dynamics of Bulk and Adsorbed Poly(methyl acrylate)-d3 by Deuterium NMR: Effect of Adsorbed Amount. *Macromolecules* **1997**, *30*, 5331−5338.

(7) Schönhoff, M.; Larsson, A.; Welzel, P. B.; Kuckling, D. Thermoreversible Polymers Adsorbed to Colloidal Silica: A 1H NMR and DSC Study of the Phase Transition in Confined Geometry. *J. Phys. Chem. B* **2002**, *106*, 7800−7808.

(8) Blum, F. D.; Krisanangkura, P. Comparison of Differential Scanning Calorimetry, FTIR, and NMR to Measurements of Adsorbed Polymers. *Thermochim. Acta* **2009**, *492*, 55−60.

(9) Moll, J.; Kumar, S. K. Glass Transitions in Highly Attractive Highly Filled Polymer Nanocomposites. *Macromolecules* **2012**, *45*, 1131−1135.

(10) Robertson, C. G.; Roland, C. M. Glass Transition and Interfacial Segmental Dynamics in Polymer-Particle Composites. *Rubber Chem. Technol.* **2008**, *81*, 506−522.

(11) Zhu, L.; Wang, X.; Gu, Q.; Chen, W.; Sun, P.; Xue, G. Confinement-Induced Deviation of Chain Mobility and Glass Transition Temperature for Polystyrene/Au Nanoparticles. *Macromolecules* **2013**, *46*, 2292−2297.

(12) Holt, A. P.; Sangoro, J. R.; Wang, Y.; Agapov, A. L.; Sokolov, A. P. Chain and Segmental Dynamics of Poly(2-vinylpyridine) Nanocomposites. *Macromolecules* **2013**, *46*, 4168−4173.

(13) Holt, A. P.; Griffin, P. J.; Bocharova, V.; Agapov, A. L.; Imel, A. E.; Dadmun, M. D.; Sangoro, J. R.; Sokolov, A. P. Dynamics at the Polymer/Nanoparticle Interface in Poly(2-vinylpyridine)/Silica Nanocomposites. *Macromolecules* **2014**, *47*, 1837−1843.

(14) Lin, C. C.; Gam, S.; Meth, J. S.; Clarke, N.; Winey, K. I.; Composto, R. J. Do Attractive Polymer−Nanoparticle Interactions Retard Polymer Diffusion in Nanocomposites? *Macromolecules* **2013**, *46*, 4502−4509.

(15) Jiang, K.; Xie, B.; Fu, D.; Luo, F.; Liu, G.; Su, Y.; Wang, D. Solid−Solid Phase Transition of n-Alkanes in Multiple Nanoscale Confinement. *J. Phys. Chem. B* **2009**, *114*, 1388−1392.

(16) Fu, D.; Su, Y.; Gao, X.; Liu, Y.; Wang, D. Confined Crystallization of n-Hexadecane Located inside Microcapsules or outside Submicrometer Silica Nanospheres: A Comparison Study. *J. Phys. Chem. B* **2013**, *117*, 6323−6329.

(17) Su, Y.; Liu, G.; Xie, B.; Fu, D.; Wang, D. Crystallization Features of Normal Alkanes in Confined Geometry. *Acc. Chem. Res.* **2014**, *1*, 192−201.

(18) Mukherjee, P. K. Tricritical Behavior of the RI−RV Rotator Phase Transition in a Mixture of Alkanes with Nanoparticles. *J. Chem. Phys.* **2011**, *135*, 134505.

(19) Zammit, U.; Marinelli, M.; Mercuri, F.; Paoloni, S.; Scudieri, F. Effect of Quenched Disorder on the RI-RV, RII-RI, and Liquid-RII Rotator Phase Transitions in Alkanes. *J. Phys. Chem. B* **2011**, *115*, 2331−2337.

(20) Kumar, M. V.; Prasad, S. K. Influence of Quenched Disorder Created by Nanosilica Network on Phase Transitions in Tetracosane. *RSC Adv.* **2012**, *2*, 8531−8538.

(21) Gang, O.; Wu, X. Z.; Ocko, B. M.; Sirota, E. B.; Deutsch, M. Surface Freezing in Chain Molecules. II. Neat and Hydrated Alcohols. *Phys. Rev. E* **1998**, *58*, 6086−6100.

(22) Sirota, E. B.; Wu, X. Z. The Rotator Phases of Neat and Hydrated 1-alcohols. *J. Chem. Phys.* **1996**, *105*, 7763−7773.

(23) Ishikawa, S.; Ando, I. Structural Studies of n-Octadecanol by Variable-Temperature Solid-State High-Resolution ^{13}C NMR Spectroscopy. *J. Mol. Struct.* **1993**, *291*, 183−190.

(24) Ocko, B. M.; Wu, X. Z.; Sirota, E. B.; Sinha, S. K.; Gang, O.; Deutsch, M. Surface Freezing in Chain Molecules: Normal Alkanes. *Phys. Rev. E* **1997**, *55*, 3164−3182.

(25) Madathingal, R. R.; Wunder, S. L. Confinement Effects of Silica Nanoparticles with Radii Smaller and Larger than Rg of Adsorbed Poly(ethylene oxide). *Macromolecules* **2011**, *44*, 2873−2882.

(26) Stöber, N.; Fink, A.; Bohn, E. Controlled Growth of Monodisperse Silica Spheres in the Micron Size Range. *J. Colloid Interface Sci.* **1968**, *26*, 62−69.

(27) Míguez, H.; Meseguer, F.; López, C.; Mifsud, A.; Moya, J. S.; Vázquez, L. Evidence of FCC Crystallization of SiO_2 Nanospheres. *Langmuir* **1997**, *13*, 6009−6011.

(28) Deng, T.; Zhang, J.; Zhu, K.; Zhang, Q.; Wu, J. Highly Monodisperse Vinyl Functionalized Silica Spheres and Their Self-Assembled Three-Dimensional Colloidal Photonic Crystals. *Colloids Surf., A* **2010**, *356*, 104−111.

(29) Rensmo, H.; Ongaro, A.; Ryan, D.; Fitzmaurice, D. Self-Assembly of Alkane Capped Silver and Silica Nanoparticles. *J. Mater. Chem.* **2002**, *12*, 2762−2768.

(30) Hao, T.; Riman, R. E. Calculation of interparticle spacing in colloidal systems. *J. Colloid Interface Sci.* **2006**, *297*, 374−377.

(31) Yamamoto, T.; Nozaki, K.; Hara, T. X-ray and Thermal Studies on the Rotator Phases of Normal Higher Alcohols $C_{17}H_{35}OH$, $C_{18}H_{37}OH$, and Their Mixtures. *J. Chem. Phys.* **1990**, *92*, 631−641.

(32) Ventolà, L.; Ramírez, M.; Calvet, T.; Solans, X.; Cuevas-Diarte, M. A.; Negrier, P.; Mondieig, D.; Van Miltenburg, J. C.; Oonk, H. A. J. Polymorphism of N-Alkanols: 1-Heptadecanol, 1-Octadecanol, 1-Nonadecanol, and 1-Eicosanol. *Chem. Mater.* **2002**, *14*, 508−517.

(33) Sirota, E. B.; King, H. E., Jr.; Shao, H. H.; Singer, D. M. Rotator Phases in Mixtures of n-Alkanes. *J. Phys. Chem.* **1995**, *99*, 798−804.

(34) Ventola, L.; Calvet, T.; Cuevas-Diarte, M. A.; Oonk, H. A. J.; Mondieig, D. Solid-Solid and Solid-Liquid Equilibria in the n-Alkanols Family: $C_{18}H_{37}OH$-$C_{20}H_{41}OH$ system. *Phys. Chem. Chem. Phys.* **2004**, *6*, 3726−3731.

(35) Henschel, A.; Huber, P.; Knorr, K. Crystallization of Medium-Length 1-Alcohols in Mesoporous Silicon: An X-ray Diffraction Study. *Phys. Rev. E* **2008**, *77*, 042602.

(36) Berwanger, R.; Henschel, A.; Knorr, K.; Huber, P.; Pelster, R. Phase Transitions and Molecular Dynamics of n-Hexadecanol Confined in Silicon Nanochannels. *Phys. Rev. B* **2009**, *79*, 125442.

(37) Maeda, N.; Yaminsky, V. V. Experimental Observations of Surface Freezing. *Int. J. Mod. Phys. B* **2001**, *15*, 3055−3077.

DOI: 10.1021/jp512124s
J. Phys. Chem. B 2015, 119, 2074−2080

(38) Ishikawa, S.; Ando, I. Structural Studies of n-Octadecanol by Variable-Temperature Solid-State High-Resolution ^{13}C NMR Spectroscopy. *J. Mol. Struct.* **1993**, *291*, 183−190.
(39) Ocko, B. M.; Hlaing, H.; Jepsen, P. N.; Kewalramani, S.; Tkachenko, A.; Pontoni, D.; Reichert, H.; Deutsch, M. Unifying Interfacial Self-Assembly and Surface Freezing. *Phys. Rev. Lett.* **2011**, *106*, 137801.

DOI: 10.1021/jp512124s
J. Phys. Chem. B 2015, 119, 2074−2080